UNVEILING THE ENVIRONMENTS OF EXTREME MASSIVE STARS

M. Kraus [a*], ***T. Liimets*** [a], ***M. L. Arias*** [b,c], ***A. Moiseev*** [d], ***L. S. Cidale*** [b,c], ***A. F. Torres*** [b,c], ***D. H. Nickeler*** [a]

[a] *Astronomical Institute, Czech Academy of Sciences, Fričova 298, 251 65 Ondřejov, Czech Republic*

[b] *Departamento de Espectroscopía, Facultad de Ciencias Astronómicas y Geofísicas, Universidad Nacional de La Plata, Paseo del Bosque S/N, La Plata, B1900FWA, Buenos Aires, Argentina*

[c] *Instituto de Astrofísica de La Plata (CCT La Plata - CONICET, UNLP) Paseo del Bosque S/N, La Plata, B1900FWA, Buenos Aires, Argentina*

[d] *Special Astrophysical Observatory, Russian Academy of Sciences, Nizhnii Arkhyz 369167, Russia*

Massive stars are powerful cosmic engines, enriching their environments with energy and mass throughout their lifetime. The post-main sequence evolution of massive stars comprises several distinct states, such as the luminous blue variables, blue supergiants, red supergiants, Wolf-Rayet stars, B[e] supergiants and yellow hypergiants, many of them connected with intense mass loss, embedding the stars in a dense environment. Here we present an overview of our studies for members in three states of evolved massive stars: B[e] supergiants, luminous blue variables, and yellow hypergiants. Combining high-quality spectral and imaging observations over large wavelength regions, we aim to unveil the physical properties and temporal evolution of the ejected material in these types of objects in order to gain insight into their mass loss and mass ejection histories. This information is also vital to constrain the location of these objects along the evolutionary path of massive stars.

Keywords: stars: massive – supergiants – circumstellar matter

* E-mail: michaela.kraus@asu.cas.cz

1. INTRODUCTION

Massive stars ($M_{\rm initial} \geq 8 M_{\odot}$) are powerful cosmic engines. Throughout their entire life they enrich their environment with huge amounts of energy and with chemically processed material, triggering the formation of next generations of stars and planets and driving the chemical evolution of their host galaxies. Despite the importance of massive stars for cosmic evolution, their aging process from the cradle up to their death in spectacular supernova explosions is most uncertain. This is due to the lack of reliable values of the total amount of mass the star loses during each epoch of its life.

The evolutionary path of massive stars comprises various extreme transition phases, in which the stars shed huge amounts of material into their environments, typically via episodic, sometimes even eruptive events. These objects are luminous supergiants or hypergiants populating the upper part of the Hertzsprung-Russell (HR) diagram and spreading from spectral type O to F or even later. Sophisticated stellar evolutionary models depend critically on the input physics. Consequently, any inaccuracy of the input parameters can result in large uncertainties of the evolutionary models [1]. As mass loss is one of the most crucial parameters for the evolution of massive stars, it is essential to understand the physical processes behind mass ejections and to properly quantify the amount they add to the total mass loss of the star within each of these evolutionary transition phases.

Some classes of evolved massive stars are particularly puzzling. These are the B[e] supergiants (B[e]SGs), the luminous blue variables (LBVs), and the yellow hypergiants (YHGs). Members of these groups are shown in Figure 1. While stars born with masses in the range $40 - 60\,M_{\odot}$ can develop into LBVs directly after they have left the main sequence, lower mass stars ($30 - 40\,M_{\odot}$) might reach this stage only in their late, post-red supergiant evolution [3]. In contrast, neither B[e]SGs nor YHGs are currently predicted by sophisticated stellar evolution models. In this work, we present the typical characteristics of these three classes of objects and a brief overview of our studies aimed to deepen our comprehension of their environments and their mass-ejection activity.

2. B[E] SUPERGIANTS

Stars classified as B[e]SGs are luminous B-type emission line stars. The best-known sample resides in the Magellanic Clouds, because these stars have precise luminosity values due to their well constrained distances. B[e]SGs in the Milky Way still face the issue of uncertain distances, although with the upcoming data release from the Gaia mission these uncertainties will hopefully decrease. The

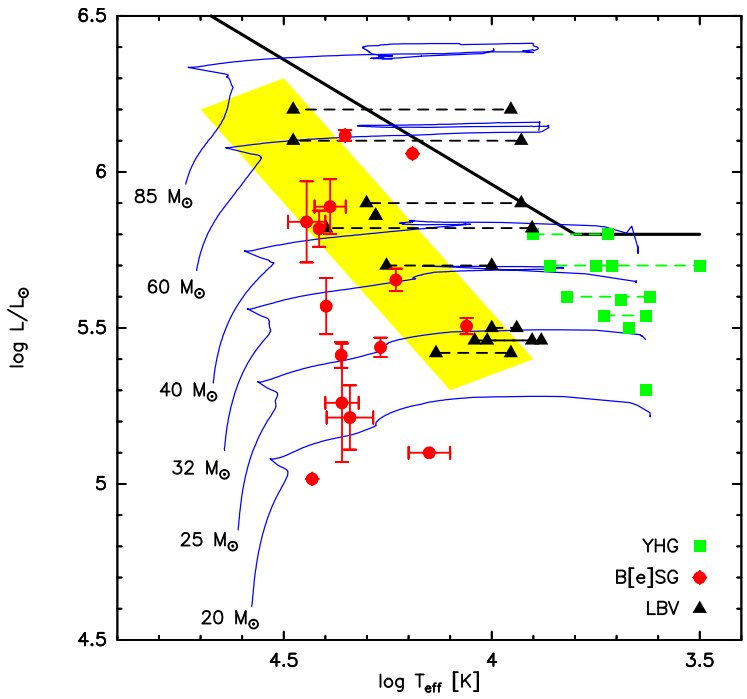

Fig. 1. HR diagram with the positions of examples of B[e]SGs, LBVs, and YHGs indicated. The thick black solid line marks the Humphreys-Davidson limit. The yellow colored domain marks the S Dor instability strip. The hot (quiescent) and cool ("outburst") positions of LBVs and YHGs are connected with dashes in the figure. Evolutionary tracks are for rotating stars at a metallicity $Z = 0.002$ and were taken from [2].

examples shown in Figure 1 are objects in the Magellanic Clouds, and their parameters have been summarized in [4] (Table 1).

The optical spectra of B[e]SGs display intense Balmer line emission along with emission from low-ionized metals such as Fe II as well as forbidden emission lines of [Fe II] and [O I]. The latter is an important classification characteristic as it is only seen in B[e]SGs, but not in other hot supergiant stars such as the LBVs.

The hybrid character of the spectra of B[e]SGs points towards an axis-symmetric wind from these stars, consisting of a hot and fast line-driven wind regime (typical for hot supergiants) in polar direction, traced by the broad P-Cygni profiles of high-ionized metals (e.g. Si IV) in ultraviolet (UV) spectra, and a much slower wind towards equatorial regions, traced by the low-ionized metal lines. A typical example is the star R 126 in the Large Magellanic Cloud (LMC). The P-Cygni absorption components in the UV indicate a polar wind with terminal velocity of about 1800 km s^{-1}, in contrast to the optical Fe II and [Fe II] lines that have full-width at half maximum values of just 20-30 km s^{-1} suggesting a much slower wind outflow [5].

Furthermore, the spectral energy distribution (SED) of B[e]SGs displays intense infrared (IR) excess emission due to hot dust [6]. Spectroscopic observations of the dust emission carried out with the *Spitzer Space Telescope* [7] revealed that the dust is composed of silicates, often enriched with polycyclic aromatic hydrocarbons (PAHs). While amorphous silicates can be expected to form in the environments of massive stars due to their oxygen-rich surface composition throughout their evolution, the presence of often crystalline silicates as well as of carbon-based dust particles is surprising, because the chemical reactions needed for their formation can happen only in stable, long-lived environments. The most logical explanation for the detected dust composition is, therefore, that the dust is confined in a circumstellar disk.

A disk structure is also supported by the high intrinsic polarization values measured from B[e]SGs [8]. These measurements agree with the idea of a density contrast between equatorial and polar regions by a factor of 100-1000. Finally, the reconstruction of interferometric observations of the Galactic B[e]SG CPD-57 2847 taken at 10 μm with the ESO instrument MIDI resulted in the first visualization of a dusty disk spreading from about 12 AU to about 130 AU [9].

2.1. Stellar environments of B[e] supergiants on small scales

The existence of stable dusty disks around B[e]SGs poses the question of their formation mechanism and their dynamics. Because dust emission has no clearly defined features that would allow to derive its kinematics, the disks need to be studied using information that can be obtained from the gas component. Assuming that the disks form from the material released from the stellar surface, then molecules should form closer to the star than the location of the inner edge of the dusty disk. And in fact, from some B[e]SG star environments emission from CO molecular bands arising in the K-band redwards of 2.293 μm has been reported [10], as well as possible emission from TiO at optical wavelengths redwards of 6160 Å [11–13].

To analyze the molecular disks around B[e]SGs in the Milky Way and in the Local Group, we have acquired near-IR spectra in medium- and high-resolution during several observing runs that have been allocated to our projects since 2009. The instruments used were SINFONI ($R \sim 4500$) and CRIRES ($R \sim 50\,000$) at ESO, along with GNIRS ($R \sim 18\,000$), Phoenix ($R \sim 50\,000$), and IGRINS ($R \sim 45\,000$) offered at Gemini Observatory. These IR data were complemented with high-resolution ($R \sim 50\,000$) optical spectra, mostly collected with the FEROS spectrograph attached to the 2.2-m Max-Planck telescope at La Silla, Chile.

Our IR survey revealed several important results. Firstly, CO band emission has been detected in only about 50% of the B[e]SGs, and these stars seem to have evolved from progenitors with initial masses in the range of $20 - 40\,M_\odot$ [4, 14]. Secondly, from our modeling of the CO emission, we found that the temperature of the molecular gas ($1900 - 3200\,K$) is, in all cases, significantly lower than the CO dissociation temperature ($\sim 5000\,K$). Because the intensity of the emission increases with the column density of the molecular gas and its temperature, the observed emission bands trace the hottest and densest molecular regions. The absence of emission that could be associated with regions having a temperature close to the dissociation temperature thus implies a lack of molecules closer to the star. Therefore, we conclude that the disks are not continuous structures spreading from the stellar surface to far distances. Instead, the emitting region is found to be confined within a detached narrow molecular ring. Finally, in all CO spectra, we also identified emission from the isotope ^{13}CO in significant amounts [14, 15]. Such intense emission can only be explained with a substantial enrichment of the circumstellar gas in ^{13}C, and this enrichment mirrors the stellar surface composition at the time of the material release [16].

Besides CO, we also detected emission from SiO in the L-band spectra of so far four Galactic B[e]SGs [17]. SiO forms at considerably lower temperatures than CO, so that SiO emission traces regions farther out than CO. The high spectral resolution of the observations allowed us to determine the kinematic broadening of both the SiO bands and the CO bands, and the dynamics retrieved from these emission bands result in the conclusion that the molecular gas is revolving around the central object on (quasi-)Keplerian orbits. Further confirmation of Keplerian rotation of the disks of B[e]SGs came from interferometric observations providing spatially resolved emission of the Brγ line [18].

The optical spectra of B[e]SGs also contain emission lines formed in the circumstellar gas disk. These are the forbidden lines of [O I] $\lambda\lambda 5577, 6300, 6364$ [19, 20], and of [Ca II] $\lambda\lambda 7291, 7324$ [21]. Of these, the [O I] 5577 Å arises from a higher energy level that requires a hotter and denser environment to be sufficiently populated. The upper levels of the two [Ca II] lines can be populated either collisionally from the ground level or via emission from the Ca II IR triplet lines. Our general observation is that the [Ca II] lines and the [O I] 5577 Å line (if present in the spectrum) display very similar profile shapes and widths, suggesting close-by (or identical) formation regions that are clearly separated from those traced by the [O I] $\lambda\lambda 6300, 6364$ lines.

Using the velocity information that is preserved in the profiles of these optically thin emission lines and combining it with the velocity information derived from the molecular gas, it is possible to trace the circumstellar disks at various distances from the star. The striking result from such analyses is that each star is

surrounded by a unique set of multiple rings or arcs of atomic and molecular gas [13,22,23], regardless of whether the star is single or part of a binary system. Out of the currently known sample of 33 B[e]SGs (plus 25 candidates), only 7 (plus 3 candidates) are confirmed binary systems. Of these, four have been studied in detail, and for three of them the rings are circumbinary, and for one of them the rings are circumprimary [22], ruling out binary interaction as the most likely disk/ring formation mechanism.

2.2. Large-scale ejecta

Besides the disks and rings on small scales with sizes of several tens of AU, B[e]SGs can also be embedded in large-scale nebulae or ejecta. The most famous object is the Galactic star MWC 137, for which a ring nebula with a diameter of 70" along its major axis has been detected during an Hα imaging survey of 25 northern Galactic B[e] stars [24]. Another B[e]SG included in that survey was MWC 349, which displays an Hα shell. In total, 12 objects of that sample were found to have nebulae.

Starting from 2018, we have carried out a new Hα imaging survey. We have complemented the original B[e] star sample with 9 northern and 23 southern objects and (re-)observed all targets using facilities of the Danish Telescope and of Gemini-South in Chile, and the Nordic Optical Telescope (NOT) and the Isaac Newton Telescope (INT) at La Palma. The aim of this survey is two-fold. On the one hand, we wish to identify more B[e] stars and B[e]SGs with nebulae or ejecta. The detection of circumstellar structures would provide clear proof for past mass ejection activity and would help placing the stars along the evolutionary path - post-red supergiants (post-RSGs) are more likely to be surrounded by expelled matter than pre-RSG objects. On the other hand, for stars with reported nebulosities we aim at detecting possible expansion or changes in nebular morphologies between the old data taken in 2001/2002 [24] and our new observations.

This imaging survey has been completed, but data analysis is still ongoing. However, we can report the detection of nebular features around $\sim$ 50% of the objects. This is very similar to the fraction reported previously from the northern sample [24]. The structures seen are spherical shells, bipolar or multipolar lobes as well as spiral-arms, bows and rings, filaments and blobs. The catalog with the images is currently in preparation for publication. But results for selected objects have already been published [25], such as for the ring nebula of MWC 137, for which our analysis revealed no measurable expansion so far [26]. However, we resolved clearly more structures inside the ring and detected a new bow-shaped feature at farther distances [27].

Furthermore, we have initiated a spectroscopic follow-up of the objects with clear nebular structures. For this, we have utilized long-slit facilities at the NOT and at the 6-m telescope of the Special Astrophysical Observatory Russian Academy of Sciences (SAO RAS) in Russia to collect spectra across individual nebular features, as well as the scanning Fabry-Perot Interferometer (FPI, [28]) at SAO RAS to map the entire nebulae in selected emission lines. The focus is on Hα and the lines of [N II] and [S II]. The aim of the spectroscopic survey is to derive information on the nebular dynamics and the physical parameters, such as the electron density distribution across the nebula. This spectroscopic survey is still ongoing, and data could be secured so far for MWC 137, for which we found that generally, the northern nebular regions are approaching while the southern ones are receding with velocities, projected to the line of sight, of more than $\pm 30\,\mathrm{km\,s^{-1}}$. But the velocities display a complex pattern across the nebular features and a stratification along the line of sight, suggesting that we observe a decrease in radial velocities from inside out that might point towards ballistic expansion. In addition, we found a very inhomogeneous electron density distribution across the entire nebula [27].

3. LUMINOUS BLUE VARIABLES

The second class of objects that we investigate are the LBVs. The classification of a star as LBV is based purely on historical grounds. These stars are luminous blue supergiants displaying specific variability in brightness and colors (see [29] for a recent review on LBVs). The most well-known variability is the so-called S Dor cycle, named after the LMC object S Doradus which has been the first object showing this phenomenon. During such a cycle, the star starts to brighten (1-2 mag) with a simultaneous reddening of its colors. At the same time, the spectral appearance changes from a hot OB-type supergiant in its quiescent stage to a cool AF-type supergiant (often referred to as "outburst"). This means that the star performs an excursion in the HR diagram from the hot to the cool side where it can reside for a significant amount of time (years to decades) before it returns to its original position and state. While its cause is still unclear, S Dor cycle activity is known only from LBVs based on which these objects can be distinguished from other evolved massive stars sharing the same location in the HR diagram. An interesting recent example of an LBV experiencing an S Dor cycle is the object RMC 40 in the Small Magellanic Cloud. It changed its spectral type from a late B/early A-type in 2002 to a late F-type supergiant in 2016 with a simultaneous brightening by more than 1 mag [30].

There is a second type of LBVs, the so-called giant eruption LBVs for which η Car is the prototype. During such eruptions, several solar masses of matter can be expelled.

In the absence of recorded S Dor cycles or a past giant eruption, it is not always easy to unambiguously classify an evolved massive star as LBV. LBVs in their hot, quiescent state share many characteristics with B[e]SGs. In particular, the optical spectra in the blue region of members of both groups are indistinguishable. Only red spectra covering the region of the [O I] and [Ca II] lines can tell the difference. Moreover, because not every B[e]SG displays CO band emission, the near-IR spectra of LBVs in quiescence and B[e]SGs can look identical as well [14]. A robust discrimination characteristic of the two groups is provided by their IR colors. We could show that LBVs and B[e]SGs clearly separate in the 2MASS $J-H$ versus $H-K$ and in the Wise $W1-W2$ versus $W2-W4$ color-color diagrams [4]. Moreover, a recent study of emission features in near-IR spectra of quiescent LBVs revealed intense emission of Mg II arising at 2.4047 and 2.4131 μm [31]. These lines are also present in the spectra of B[e]SGs, but with significantly lower intensity. We note, that the presence of intense Mg II lines is a weak classification criterion, but combined with the ones mentioned before, it supported the classification of some LBV candidates, e.g., the Galactic object MN 112 [31]. This object has recently been confirmed as a dormant LBV [32] due to its inactivity for more than a century.

3.1. Nebulae of LBVs

Many LBVs are surrounded by large-scale nebulae detected on optical images taken in Hα or in the nebular lines of [N II]. The high mass loss of LBVs in relation with the change in wind conditions during an S Dor cycle leads to wind-wind interaction and consequently to circumstellar structures of swept-up wind material. On the other hand, giant eruptions result in large-scale ejecta. A systematic survey of the nebular structures revealed that their morphology encompasses ring-like shells or triple-ring systems, while about 50% of the LBV nebulae have bipolar lobes [33].

Based on IR archival data retrieved with the *Spitzer Space Telescope*, a great number of IR nebulae have been discovered that host massive stars, many of which have been suggested to be LBV candidates (e.g., [34]). We have already imaged two of them in Hα to search for optical counterparts of their IR nebulae. These are the Galactic objects MN 83 and MN 112. Only MN 112 shows large-scale diffuse emission, whereas no emission has been detected from the environment of MN 83 [31]. However, the extinction we derived towards the latter object is with $A_{\rm V} > 20$ mag much too high to be able to detect any optical signal.

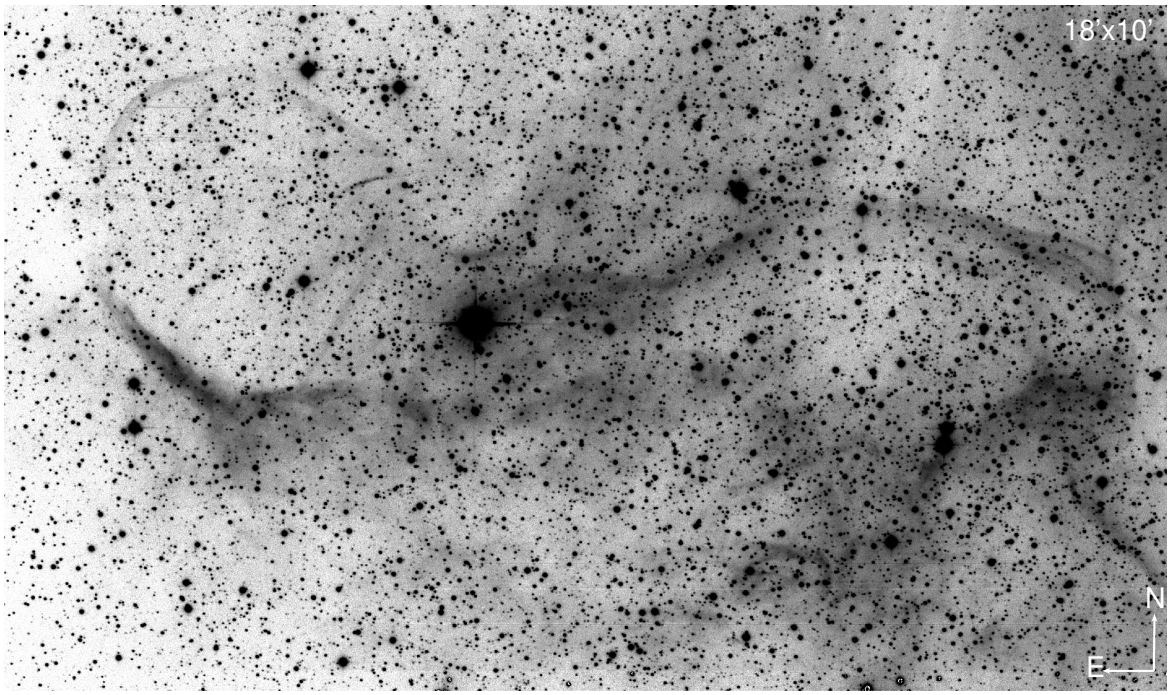

Fig. 2. Hα image of the large-scale bipolar nebula of the LBV candidate MWC 314 taken with the INT. The total extent in east-west direction corresponds to 13.2 pc.

Apart from searching for optical counterparts, we also started a detailed investigation of the large-scale bipolar nebula of the Galactic object MWC 314 (Figure 2). It has the status of an LBV candidate (e.g., [35] and references therein), and its nebula has a total extent of 13.2 pc considering a distance of 3 kpc [24]. No measurable expansion of the nebular structures could be detected when comparing Hα images taken 18 years apart [25]. We have mapped the kinematics of the nebula in Hα using the FPI at SAO in its scanning mode. The analysis of these observations is still ongoing, but first estimates suggest that the southern nebular domains are approaching and the northern ones are receding with maximum values of $\pm 40\,\mathrm{km\,s^{-1}}$ [25]. This low velocity explains the non-detection of an expansion on the images so far. Follow-up observations with the FPI in the [S II] lines to retrieve the electron density distribution across the nebula are already planned. Furthermore, the surrounding of the nebula is being observed with APEX in the lines of CO(2-1), ^{13}CO(2-1), and C^{18}O(2-1). These observations will provide physical parameters such as kinematics, density and temperature, in both the shocked gas at the rims of the bipolar nebula and in the ambient medium, needed to constrain the mass ejection history and the interaction of the ejecta with the ambient interstellar medium.

4. YELLOW HYPERGIANTS

Finally we turn to the YHGs. This class encompasses objects with temperatures of $T_{\rm eff} = 4000-7000\,{\rm K}$ and luminosities of $\log L/L_\odot = 5.4-5.8$. This rather narrow luminosity interval translates into a range of initial masses of $20-40\,{\rm M}_\odot$ for the progenitor stars. YHGs were proposed to be in their post-RSG evolutionary phase [36]. As such, they have lost a considerable amount of mass during the previous RSG phase. Due to this mass loss, the luminosity over mass ratio of YHGs can easily exceed the critical value of $\log(L_*/M_*) = 4$ (in solar units), above which the strongly inflated envelopes become unstable.

The light curves of YHGs display cyclic, but not strictly periodic variability, which seems to be related to (radial) pulsation activity. Small perturbations within the envelope can develop velocity amplitudes within the outer atmospheric layers exceeding the escape velocity and hence leading to enhanced mass loss or to mass ejections in the form of outbursts. As a result, YHGs can be surrounded by multiple shells of gas and dust. An impressive example is the southern object IRAS 17163-3907. It must have experienced at least three outbursts during the past 100 yr resulting in three distinct dust shells [37]. The appearance of IRAS 17163-3907 and its surrounding dust shells on IR images earned it the nickname 'Fried Egg Nebula' [38]. An outburst is usually accompanied by an apparent drop in temperature so that the star shifts to a cooler (redder) position in the HR diagram. As soon as the ejected material expanded and diluted, the star appears back at its previous position. These excursions in the HR diagram are marked in Figure 1 by the connecting lines between the original (warm) and the outburst (cool) locations.

The dust formed from the ejected matter can be traced by its IR excess emission in the SED. An intense IR excess emission has been detected from the Fried Egg Nebula [37] whereas less pronounced emission is seen from three YHGs in the LMC [39]. Nevertheless, the circumstellar matter of the LMC objects is warm and dense enough for molecules to form in substantial amounts, but intense molecular emission from CO has only been detected from two objects [14].

In the northern sky only four Galactic YHGs are currently known, and we spectroscopically monitor them since 2010 with the Perek 2-m telescope at Ondřejov Observatory. Of these, ρ Cas is famous for its outburst activity [40]. The most recent one took place in 2013, during which the brightness decreased by 0.6 mag and we noted a simultaneous drop of the star's temperature by 3000 K. Furthermore, the spectral lines clearly displayed an enhanced pulsation activity in the star's atmosphere prior to the outburst [41]. This has been the fourth recorded event during the past 80 yr. Although it turned out to be less pronounced than its progenitors [42], the time interval between the outbursts steadily decreases, sug-

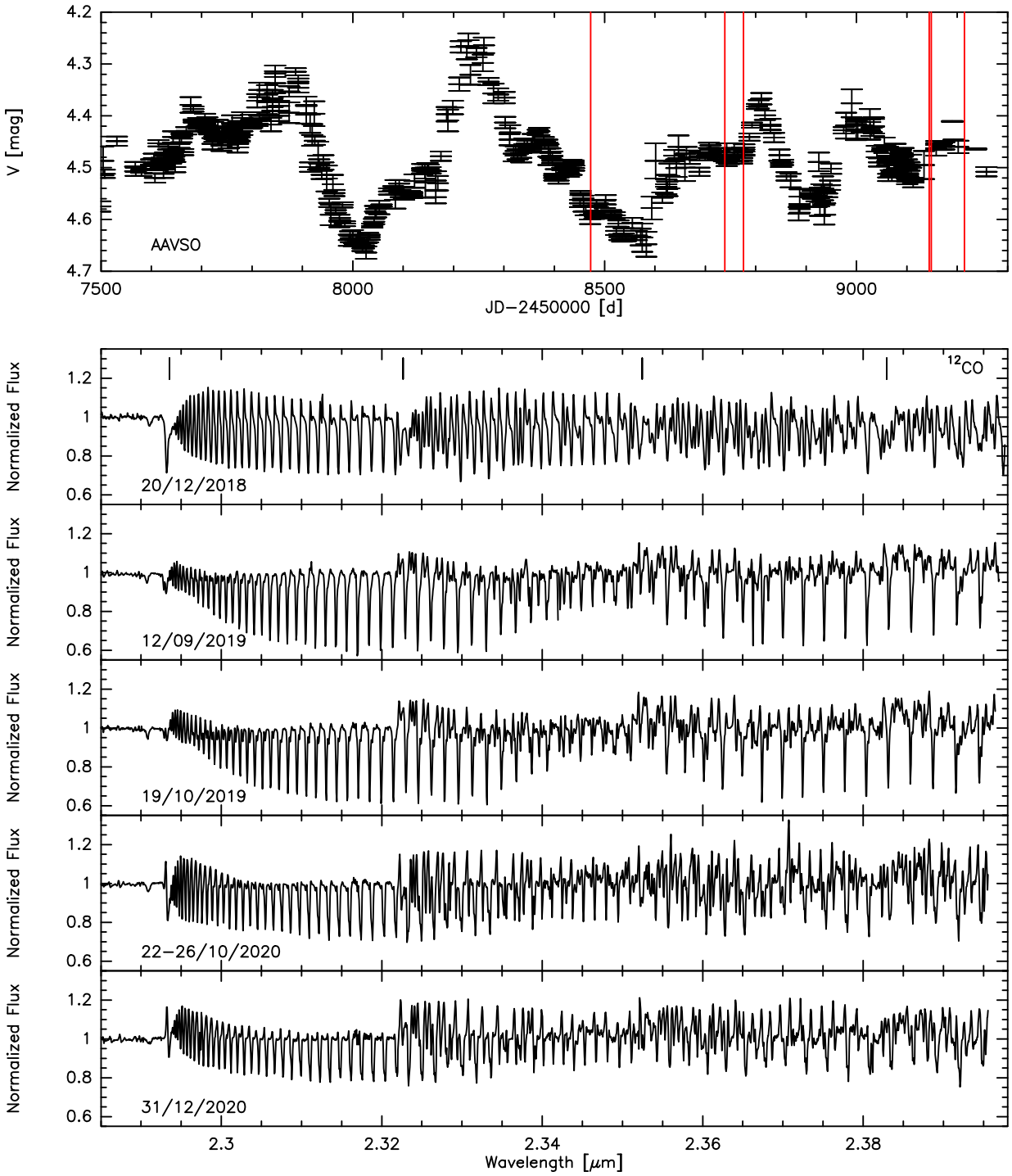

Fig. 3. Top: Light curve of ρ Cas in the years 2016-2021 taken from AAVSO. Red lines mark the dates of the IR observations. **Bottom:** K-band spectra of ρ Cas covering the CO band region at different epochs. The spectra have been obtained with GNIRS at GEMINI-North with a resolution of $R \sim 18\,000$ (IDs: GN-2018B-Q-410, GN-2019B-Q-405, GN-2020B-Q-408).

gesting that the star still has a rather unstable envelope and more mass ejection episodes might be expected in the near future.

So far, it seems that only the eruption that took place in 1946 ejected sufficient material to create detectable dust emission. Since then, this matter is expanding and diluting [43]. However, our careful analysis of the optical spectra revealed static emission in the low-excitation neutral iron line at 6359 Å as well as in the line of [CaII] at 7324 Å [41]. Furthermore, emission from CO has been detected [44], especially during phases of maximum brightness, which correspond to phases of highest temperature. In other phases, the circumstellar emission component is polluted with intense photospheric CO absorption.

We have initiated a K-band monitoring campaign with GNIRS at Gemini-North (PI: M.L. Arias) to investigate the physical conditions within the CO emitting circumstellar envelope. So far, we could collect five sets of spectra distributed from December 2018 to December 2020. These are shown in the lower panels of Figure 3. The CO bands display clear variability and changes between emission and absorption. The dates of the observations are marked in the light curve that is shown in the top panel of Figure 3. The photometric data cover the period from 2016-2021 and have been taken from the AAVSO database[1)]. Due to the highly irregular light curve variability, it is difficult to predict the next epoch with maximum brightness, and so far we have been unlucky and our K-band observations fall all on dates with intermediate brightness. Nevertheless, the analysis of the CO band spectra is work in progress, and we expect to gain from them deeper comprehension about the dynamics and physical conditions within the outermost photospheric layers of this fascinating object.

5. CONCLUSIONS

We have presented an overview of our research related to massive stars in three distinct states: B[e]SGs, LBVs, and YHGs, representative for classes of extreme massive stars. Members of these classes display outburst activities and/or phases of enhanced non-spherical mass loss, and the released material can be traced both on small (circumstellar rings and disks with extents of a few dozens of AU) as well as on large scales (with sizes of several pc) around the objects. Utilizing high-quality multi-wavelength spectroscopic and imaging data we were able to constrain physical properties of the ejected matter, such as the dynamics, temperature and density distributions in diverse physical states (atomic and molecular gas, and dust).

As a final remark, we wish to address the fact that B[e]SGs, LBVs, and YHGs populate a domain in the HR diagram in which stars are generally unstable to non-adiabatic radial pulsations. Such pulsations can develop the right power to

[1)] https://www.aavso.org/

drive mass loss [45] and even trigger mass eruptions [46]. Theoretical investigations of such pulsation instabilities for our extreme massive stars are work in progress. In case these pulsations turn out to be capable of causing mass loss in amounts similar to the observed values, these instabilities might become the key "missing-link" for understanding the physics behind outbursts and mass ejection events from evolved massive stars. The results from such investigations might then contribute significant, complementary mass-loss rates as input into sophisticated stellar evolution models. These mass-loss rates are crucial for reliable predictions of the final fate of massive stars.

Acknowledgements MK wishes to thank the organizers of the conference for their kind invitation to present this overview. MK, TL, and DHN acknowledge financial support from GA ČR (grant number 20-00150S). The Astronomical Institute Ondřejov is supported by the project RVO:67985815. MLA and AFT acknowledge financial support from CONICET (PIP 1337), and the Universidad Nacional de La Plata (Programa de Incentivos 11/G160), Argentina. This project has received funding from the European Union's Framework Programme for Research and Innovation Horizon 2020 (2014-2020) under the Marie Skłodowska-Curie Grant Agreement No. 823734.

REFERENCES

1. Martins F., Palacios A., 2013, A comparison of evolutionary tracks for single Galactic massive stars., A&A., 560, **16**, 16

2. Georgy C., Ekström S., Eggenberger P., et al., 2013, Grids of stellar models with rota- tion. III. Models from 0.8 to 120 $M_{\odot}$ at a metallicity Z = 0.002., A&A., 558, **103**, 17

3. Meynet G., Georgy C., Hirschi R., et al., 2011, Red Supergiants, Luminous Blue Vari- ables and Wolf-Rayet stars: the single massive star perspective., Société Royale des Sciences de Liège., Bulletin., **80**, 266

4. Kraus M., 2019, A Census of B[e] Supergiants., Galaxies., 7, **83**, 36

5. Zickgraf F.J., Wolf B., Stahl O., et al., 1986, The hybrid spectrum of the LMC hypergiant R 126., A&A., **143**, 421

6. Zickgraf F.J., Wolf B., Stahl O., et al., 1986, B(e)-supergiants of the Magellanic Clouds., A&A., **163**, 119

7. Kastner J.H., Buchanan C., Sahai R., et al., 2010, The Dusty Circumstellar Disks of B[e] Supergiants in the Magellanic Clouds., AJ. **139**, 1993

8. Melgarejo R., Magalh˜aes A.M., Carciofi A.C., et al., 2001, S 111 and the polarization of the B[e] supergiants in the Magellanic Clouds., A&A., **377**, 581

9. Domiciano de Souza A., Bendjoya P., Niccolini G., et al., 2011, Fast ray-tracing algorithm for circumstellar structures (FRACS). II. Disc parameters of the B[e] supergiant CPD-57° 2874 from VLTI/MIDI data., A&A., 525, **22**, 11

10. McGregor P.J., Hillier D.J., Hyland A.R., 1988, CO Overtone Emission from Magellanic Cloud Supergiants., Ap.J, **334**, 639.

11. Zickgraf F.-J., Wolf B., Stahl O., Humphreys R.M., 1989, S 18: a new B(e) supergiant in the Small Magellanic Cloud with evidence for an excretion disk., A&A., **220**, 206

12. Torres A.F., Kraus M., Cidale L.S., et al., Discovery of Raman-scattered lines in the massive luminous emission-line star LHA 115-S 18. 2012, MNRAS, **427**, L80-L84.

13. Kraus M., Cidale L.S., Arias M.L., et al., 2016, Inhomogeneous molecular ring around the B[e] supergiant LHA 120-S 73., A&A., 593, **112**, 14

14. Oksala M.E., Kraus M., Cidale L. S., 2013, et al., Probing the ejecta of evolved massive stars in transition. A VLT/SINFONI K-band survey., A&A., 558, **17**, 20

15. Liermann A., Kraus M., Schnurr O., Borges Fernandes M., 2010, The^{13}Carbon footprint of B[e] supergiants., MNRAS, **408**, 6

16. Kraus M., 2009, The pre- versus post-main sequence evolutionary phase of B[e] stars. Constraints from ^{1}3CO band emission., A&A., **494**, 253

17. Kraus M., Oksala M.E., Cidale L.S., et al., 2015, Discovery of SiO Band Emission from Galactic B[e] Supergiants., Ap.J. Letters, 800, **20**, 5

18. Millour F., Meilland A., Chesneau O., et al., 2011, Imaging the spinning gas and dust in the disc around the supergiant A[e] star HD 62623., A&A., 526, **107**, 8

19. Kraus M., Borges Fernandes M., de Araújo F.X., 2007, On the hydrogen neutral out- flowing disks of B[e] supergiants., A&A., **463**, 627

20. Kraus M., Borges Fernandes M., de Araújo F.X., 2010, Neutral material around the B[e] supergiant star LHA 115-S 65: An outflowing disk or a detached Keplerian rotating disk., A&A 517, **30**, 13

21. Aret A., Kraus M., Muratore M.F., 2012 ,Borges Fernandes M., A new observational tracer for high- density disc-like structures around B[e] supergiants., MNRAS, **423**, 284

22. Maravelias G., Kraus M., Cidale L.S., et al., 2018, Resolving the kinematics of the discs around Galactic B[e] supergiants., MNRAS, **480**, 320

23. Torres A.F., Cidale L.S., Kraus M., et al., 2018, Resolving the clumpy circumstellar environment of the B[e] supergiant LHA 120-S 35., A&A., 612, **113**, 16

24. Marston A.P., McCollum B., 2008, Extended shells around B[e] stars. Implications for B[e] star evolution., A&A., 477, 193

25. Liimets T., Kraus M., Moiseev A., et al., 2022, Follow-Up of Extended Shells around B[e] Stars., Galaxies., 10, **41**, 11

26. Kraus M., Liimets T., Cappa C.E., et al., 2017, Resolving the Circumstellar Environ- ment of the Galactic B[e] Supergiant Star MWC 137 from Large to Small Scales., AJ, 154, **186**, 19

27. Kraus M., Liimets T., Moiseev A., et al., 2021, Resolving the Circumstellar Environment of the Galactic B[e] Supergiant Star MWC 137. II. Nebular Kinematics and Stellar Variability., AJ, 162, **150**, 14

28. Moiseev A.V., 2021, Scanning Fabry-Perot Interferometer of the 6-m SAO RAS Tele- scope., Astrophys.Bull., **76**, 316

29. Weis K., Bomans D.J., 2020, Luminous Blue Variables., Galaxies., 8, **20**, 29

30. Campagnolo J.C.N., Borges Fernandes M., Drake N.A., et al., 2018, Detection of new eruptions in the Magellanic Clouds luminous blue variables R 40 and R 110. 2018, A&A., 613, **33**, 24

31. Cochetti Y.R., Kraus M., Arias M.L., et al., 2020, Near-infrared Characterization of Four Massive Stars in Transition Phases., AJ, 160, **166**, 10

32. Maryeva O.V., Karpov S.V., Kniazev A.Y., et al., 2022, How long can luminous blue vari- ables sleep? A long-term photometric variability and spectral study of the Galactic candidate luminous blue variable MN 112., MNRAS, **513**, 5752

33. Weis K., 2011, Nebulae around Luminous Blue Variables - large bipolar variety. Active OB stars: structure, evolution, mass loss, and critical limits., C. Neiner, G. Wade, G. Meynet, G. Peters (Eds.), IAU Symposium., **272,** 372

34. Gvaramadze V.V., Kniazev A.Y. Fabrika S., 2010, Revealing evolved massive stars with Spitzer., MNRAS, **405**, 1047

35. Liermann A., Schnurr O., Kraus M., 2014, et al., A K-band mini-survey of Galactic B[e] stars., MNRAS, **443**, 947

36. de Jager C., 1988, The yellow hypergiants., A&A., **8**, 145

37. Koumpia E., Oudmaijer R.D., Graham V., et al., 2020, Optical and near-infrared ob- servations of the Fried Egg Nebula. Multiple shell ejections on a 100 yr timescale from a massive yellow hypergiant., A&A., 635, **183**, 24

38. Lagadec E., Zijlstra A.A., Oudmaijer R.D., et al., 2011, A double detached shell around a post-red supergiant: IRAS 17163-3907, the Fried Egg nebula., A&A., 534, **10,** 4

39. Kourniotis M., Kraus M., Maryeva O., et al., 2022, Revisiting the evolved hypergiants in the Magellanic Clouds., MNRAS, **511**, 4360

40. Lobel A., Dupree A.K., Stefanik R.P., et al., 2003, High-Resolution Spectroscopy of the Yellow Hypergiant ρ Cassiopeiae from 1993 through the Outburst of 2000-2001., Ap.J., **583**, 923

41. Kraus M., Kolka I., Aret A., et al., 2019, A new outburst of the yellow hypergiant star ρ Cas., MNRAS, **483**, 3792

42. Maravelias G., Kraus M., 2022, Bouncing against the Yellow Void-Exploring the Out- bursts of ρ Cassiopeiae from Visual Observations., JAAVSO, 50, **49**, 7

43. Shenoy D., Humphreys R.M., Jones T.J., et al., 2016, Searching for Cool Dust in the Mid-to-far Infrared: The Mass-loss Histories of the Hypergiants μ Cep, VY CMa, IRC+10420, and ρ Cas., AJ, 151, **51**, 14

44. Gorlova N., Lobel A., Burgasser A.J., et al., 2006, On the CO Near-Infrared Band and the Line-splitting Phenomenon in the Yellow Hypergiant ρ Cassiopeiae., Ap.J., **651**, 1130

45. Yadav A.P., Glatzel W., 2016, Stability analysis, non-linear pulsations and mass loss of models for 55 Cygni (HD 198478)., MNRAS, **457**, 4330

46. Glatzel W., Kiriakidis M., Chernigovskij S., Fricke K.J., 1999, The non-linear evolution of strange-mode instabilities., MNRAS, **303**, 116